



# Click modification of azo-containing polyurethanes through polymer reaction: Convenient, adjustable structure and enhanced nonlinear optical properties

Zhong'an Li<sup>a</sup>, Wenbo Wu<sup>a</sup>, Pan Hu<sup>a</sup>, Xiaojun Wu<sup>a</sup>, Gui Yu<sup>b</sup>, Yunqi Liu<sup>b</sup>, Cheng Ye<sup>b</sup>, Zhen Li<sup>a,\*</sup>, Jingui Qin<sup>a</sup>

<sup>a</sup> Department of Chemistry, Wuhan University, Wuhan 430072, China

<sup>b</sup> Institute of Chemistry, Chinese Academy of Sciences, Beijing 100080, China

## ARTICLE INFO

### Article history:

Received 29 July 2008

Received in revised form

25 October 2008

Accepted 27 October 2008

Available online 5 November 2008

### Keywords:

Nonlinear optical polyurethanes

Post-functionalization

Click chemistry

Synthesis

Isolation groups

Structural modification

## ABSTRACT

Eight novel polyurethanes with adjustable structures were prepared from two basic polymers; the compounds displayed good solubility in common organic solvents and high thermal stability. The presence of terminal alkyne moieties further improved the thermal stability of the polymers. The resonant  $d_{33}$  values of the polymers could be improved up to 1.55 times by attaching suitable isolation spacers, with the achieved highest  $d_{33}$  value to be 94.4 pm/V.

© 2008 Elsevier Ltd. All rights reserved.

## 1. Introduction

"Click" chemistry has aroused much interest among researchers because of its remarkable features such as nearly quantitative yields, mild reaction conditions, broad tolerance toward functional groups, low susceptibility to side reactions, and simple product isolation. The click-chemistry strategy has been successfully applied to macromolecular chemistry, affording polymeric materials varying from block copolymers, dendrimers, to complex macromolecular structures. Among "click" chemistry reactions, the copper catalyzed Huisgen cycloaddition, also termed as the Sharpless "click" reaction, is the typical example, and has been widely utilized in different research fields [1–20]. Just using this reaction, we could conveniently prepare disubstituted polyacetylenes (PAs) bearing polar azo moieties in the side chains [21], which were inaccessible from their corresponding monomers, although lots of PAs could be obtained from the polymerization of the monomers directly. Also, we have easily synthesized a series of small azo chromophore molecules with different isolation groups through this reaction [22]. These successful cases prompted us to solve other synthetic problems encountered by using the "Click" chemistry reaction.

Recently, on the basis of the published work, we have tried to explore some approaches to partially solve one of the major problems encountered in optimizing organic second-order nonlinear optical (NLO) materials [23–25]: to efficiently translate the large  $\beta$  values of the organic chromophores into high macroscopic NLO activities of polymers, according to the site isolation principle [26]. Our research demonstrated that the macroscopic nonlinearity of NLO polymers could be boosted much higher by bonding "suitable isolation groups" to the NLO chromophore moieties [27–33]. And in our previous cases, we first prepared the designed NLO chromophores with different isolation groups, introduced these chromophores to polymers through the polymerization process or post-functional polymer reactions, then studied the NLO properties of the resultant NLO polymers. This strategy, in a large extent, caused the synthetic difficulty. It was also decided to modify the NLO character of preferred polymers by attaching a "suitable isolation group" through polymer reaction so as to adjust the subtle structure of NLO polymers to determine their NLO properties. Thus, partially based on our previous work [34,35], especially the usage of "Click" chemistry [21,22,30], in this paper, we reported such examples: different isolation groups could be linked to the chromophore moieties on polymer side chains conveniently, to modify their NLO properties (Schemes 1 and 2). As shown, **P2–P5** and **P7–P10** could be easily derived from their mother polymers (**P1** and **P6**), through polymer reactions by using

\* Corresponding author. Tel.: +86 27 62254108; fax: +86 27 68756757.

E-mail address: [lizhen@whu.edu.cn](mailto:lizhen@whu.edu.cn) (Z. Li).



“Click” chemistry. All the polymers were well characterized, showed good performance, and might be good candidates for the practical applications. Herein, we would like to report their syntheses and NLO properties in detail.

## 2. Experimental section

### 2.1. Materials

*N,N*-Dimethylformamide (DMF) was dried over and distilled from  $\text{CaH}_2$  under an atmosphere of dry nitrogen. Toluene 2,4-diisocyanate (TDI) was purified by distillation under reduced pressure before use. *N,N,N',N'*-Pentamethyldiethylenetriamine (PMDETA) was purchased from Alfa Aesar. The synthesis of chromophores **1** and **6** was according to our previous work [30]. All other reagents were used as-received.

### 2.2. Instrumentation

$^1\text{H}$  spectra were measured on a Varian Mercury300 spectrometer using tetramethylsilane (TMS;  $\delta = 0$  ppm) as internal standard. The Fourier transform infrared (FT-IR) spectra were recorded on a Perkin Elmer-2 spectrometer in the region of  $3000\text{--}400\text{ cm}^{-1}$  on NaCl pellets. UV-vis spectra were obtained using a Shimadzu UV-2550 spectrometer. GPC analysis was performed on an Agilent 1100 series HPLC system and a G1362A refractive index detector. Polystyrene standards were used as calibration standards for GPC. THF was used as an eluent and the flow rate was  $1.0\text{ mL/min}$ . Thermal analysis was performed on NETZSCH STA449C thermal analyzer at a heating rate of  $10\text{ }^\circ\text{C/min}$  in nitrogen at a flow rate of  $50\text{ cm}^3/\text{min}$  for thermogravimetric analysis (TGA). The thermal transitions of the polymers were investigated using a METTLER differential scanning calorimeter DSC822e under nitrogen at a scanning rate of  $10\text{ }^\circ\text{C/min}$ . The thermometer for measurement of the melting point was uncorrected. The thickness of the films was measured with an Ambios Technology XP-2 profilometer.

### 2.3. General procedure for the synthesis of alkyne-containing polyurethanes **P1** and **P6** (Schemes 1 and 2)

Chromophore **1** or **6** and TDI with equivalent molar ratios were reacted in appropriate anhydrous DMF solution at  $80\text{ }^\circ\text{C}$  for 30 h under an atmosphere of dry nitrogen. After the solution was cooled to ambient temperature, it was dropped into methanol to remove monomers. The polymer was filtered and dried in a vacuum desiccator.

**Polymer P1.** **1** (0.82 g, 1.98 mmol), TDI (0.36 g, 1.98 mmol). Polymer **P1** was obtained as a deep red powder (1.01 g, 85.6%).  $M_w = 15\,000$ ,  $M_w/M_n = 1.49$  (GPC, polystyrene calibration). IR (thin film),  $\nu$  ( $\text{cm}^{-1}$ ): 1723 (C=O), 1517, 1340 ( $-\text{NO}_2$ ).  $^1\text{H}$  NMR ( $\text{DMSO}-d_6$ )  $\delta$  (ppm): 1.9–2.2 ( $-\text{CH}_3$ ,  $-\text{CH}_2-$  and  $\equiv\text{C}-\text{H}$ ), 2.4 ( $-\text{CH}_2-$ ), 3.7–3.9 ( $-\text{N}-\text{CH}_2-$ ), 4.2–4.4 ( $-\text{O}-\text{CH}_2-$ ), 6.8–7.2 (ArH), 7.5 (ArH), 7.6 (ArH), 7.7–8.0 (ArH), 8.8–9.0 ( $-\text{NH}-$ ), 9.4–9.6 ( $-\text{NH}-$ ).  $^{13}\text{C}$  NMR ( $\text{DMSO}-d_6$ )  $\delta$  (ppm): 13.33, 15.10, 17.72, 28.38, 50.15, 61.97, 68.67, 72.12, 72.36, 84.21, 110.27, 112.50, 116.12, 117.14, 117.89, 123.80, 125.98, 126.43, 130.95, 136.90, 137.36, 137.64, 144.61, 147.16, 148.53, 152.17, 154.08, 154.87, 155.09, 155.32. UV-vis (DMF, 0.02 mg/mL):  $\lambda_{\text{max}}$  (nm): 484.

**Polymer P6.** **6** (0.62 g, 1.50 mmol), TDI (0.27 g, 1.50 mmol). Polymer **P6** was obtained as an orange red powder (0.79 g, 88.3%).  $M_w = 8200$ ,  $M_w/M_n = 1.60$  (GPC, polystyrene calibration). IR (thin film),  $\nu$  ( $\text{cm}^{-1}$ ): 1719 (C=O), 1317, 1130 ( $-\text{SO}_2$ ).  $^1\text{H}$  NMR ( $\text{DMSO}-d_6$ )  $\delta$  (ppm): 1.6–1.8 ( $-\text{CH}_2-$ ), 1.9–2.2 ( $-\text{CH}_3$  and  $\equiv\text{C}-\text{H}$ ), 2.3 ( $-\text{CH}_2-$ ), 3.4 ( $-\text{SO}_2\text{CH}_2-$ ), 3.7–3.9 ( $-\text{N}-\text{CH}_2-$ ), 4.2–4.4 ( $-\text{O}-\text{CH}_2-$ ), 6.9–7.2 (ArH), 7.5 (ArH), 7.7–7.8 (ArH), 7.8–8.0 (ArH), 8.8–9.0 ( $-\text{NH}-$ ), 9.4–9.5 ( $-\text{NH}-$ ).  $^{13}\text{C}$  NMR ( $\text{DMSO}-d_6$ )  $\delta$  (ppm): 13.34, 17.07, 17.75, 22.54, 50.16, 54.58, 61.96, 72.95, 83.50, 112.51, 116.06, 123.16, 126.00,

126.42, 129.79, 130.98, 136.92, 137.36, 137.65, 139.15, 143.78, 152.24, 154.10, 154.90, 155.11, 156.16. UV-vis (DMF, 0.02 mg/mL):  $\lambda_{\text{max}}$  (nm): 446.

### 2.4. General procedure for the synthesis of polyurethanes **P2–P5** and **P7–P10**

A mixture of alkyne-containing polymer **P1** or **P6** (1.00 equiv), azide-containing compound (one of **2–5**) (1.10–1.20 equiv), and CuBr (1.00 equiv) was dissolved in DMF (0.1 M of alkyne) under nitrogen in a Schlenk flask, then *N,N,N',N'*-Pentamethyldiethylenetriamine (PMDETA) (1.00 equiv) was added. After stirred at  $25\text{--}30\text{ }^\circ\text{C}$  for 3 h, the reaction was stopped, and the resultant mixture was dropped into a lot of methanol. The polymer was obtained by filtration, and dried in a vacuum desiccator.

**Polymer P2.** Polymer **P1** (89 mg), **2** (21 mg, 0.17 mmol). Deep red powder (99 mg, 91.6%).  $M_w = 12\,000$ ,  $M_w/M_n = 1.69$  (GPC, polystyrene calibration). IR (thin film),  $\nu$  ( $\text{cm}^{-1}$ ): 1716 (C=O), 1518, 1337 ( $-\text{NO}_2$ ).  $^1\text{H}$  NMR ( $\text{DMSO}-d_6$ )  $\delta$  (ppm): 0.7–0.8 ( $-\text{CH}_3$ ), 1.0–1.2 ( $-\text{CH}_2\text{CH}_2-$ ), 1.6–1.8 ( $-\text{CH}_2-$ ), 1.9–2.2 ( $-\text{CH}_2-$  and  $-\text{CH}_3$ ), 2.7–2.9 ( $-\text{CH}_2-\text{C}-$ ), 3.7–3.9 ( $-\text{N}-\text{CH}_2-$ ), 4.1–4.4 ( $-\text{O}-\text{CH}_2-$  and  $-\text{N}-\text{CH}_2-$ ), 6.9–7.2 (ArH), 7.4–7.5 (ArH), 7.5–7.6 (ArH), 7.7–8.0 (ArH), 8.8–9.0 ( $-\text{NH}-$ ), 9.4–9.5 ( $-\text{NH}-$ ).  $^{13}\text{C}$  NMR ( $\text{DMSO}-d_6$ )  $\delta$  (ppm): 13.29, 14.38, 17.69, 22.09, 22.51, 26.12, 28.96, 30.24, 31.18, 49.83, 50.15, 61.96, 69.32, 110.03, 112.51, 116.10, 116.99, 117.83, 122.50, 123.80, 125.97, 126.47, 128.15, 130.92, 136.90, 137.35, 137.65, 144.59, 147.08, 148.51, 152.12, 154.07, 154.89, 155.10, 155.42. UV-vis (DMF, 0.02 mg/mL):  $\lambda_{\text{max}}$  (nm): 485.

**Polymer P3.** Polymer **P1** (89 mg), **3** (24 mg, 0.18 mmol). Deep red powder (95 mg, 87.2%).  $M_w = 11\,200$ ,  $M_w/M_n = 1.70$  (GPC, polystyrene calibration). IR (thin film),  $\nu$  ( $\text{cm}^{-1}$ ): 1716 (C=O), 1518, 1338 ( $-\text{NO}_2$ ).  $^1\text{H}$  NMR ( $\text{DMSO}-d_6$ )  $\delta$  (ppm): 1.9–2.2 ( $-\text{CH}_2-$  and  $-\text{CH}_3$ ), 2.7–2.9 ( $-\text{CH}_2-\text{C}-$ ), 3.7–3.9 ( $-\text{N}-\text{CH}_2-$ ), 4.1–4.3 ( $-\text{O}-\text{CH}_2-$ ), 5.4–5.6 ( $-\text{CH}_2\text{Ph}$ ), 6.8–7.1 (ArH), 7.1–7.3 (ArH), 7.4 (ArH), 7.5–7.6 (ArH), 7.7–8.0 (ArH), 8.8–9.0 ( $-\text{NH}-$ ), 9.4–9.6 ( $-\text{NH}-$ ).  $^{13}\text{C}$  NMR ( $\text{DMSO}-d_6$ )  $\delta$  (ppm): 13.34, 17.72, 22.08, 28.92, 50.13, 53.36, 61.94, 69.30, 110.09, 112.49, 116.04, 116.99, 117.84, 122.87, 123.38, 125.96, 126.43, 128.40, 128.62, 129.30, 130.95, 136.80, 137.34, 137.64, 144.59, 147.06, 148.51, 152.10, 154.06, 154.86, 155.08, 155.38. UV-vis (DMF, 0.02 mg/mL):  $\lambda_{\text{max}}$  (nm): 485.

**Polymer P4.** Polymer **P1** (89 mg), **4** (40 mg, 0.17 mmol). Deep red powder (105 mg, 84.0%).  $M_w = 12\,800$ ,  $M_w/M_n = 1.40$  (GPC, polystyrene calibration). IR (thin film),  $\nu$  ( $\text{cm}^{-1}$ ): 1723 (C=O), 1515, 1337 ( $-\text{NO}_2$ ).  $^1\text{H}$  NMR ( $\text{DMSO}-d_6$ )  $\delta$  (ppm): 1.9–2.2 ( $-\text{CH}_2-$  and  $-\text{CH}_3$ ), 2.83 ( $-\text{CH}_2-\text{C}-$ ), 3.8 ( $-\text{N}-\text{CH}_2-$ ), 4.0–4.1 ( $-\text{O}-\text{CH}_2-$ ), 4.2–4.4 ( $-\text{O}-\text{CH}_2-$  and  $-\text{N}-\text{CH}_2-$ ), 6.7–7.2 (ArH), 7.3–7.6 (ArH), 7.6–8.0 (ArH), 8.1 (ArH), 8.8–9.0 ( $-\text{NH}-$ ), 9.5–9.6 ( $-\text{NH}-$ ).  $^{13}\text{C}$  NMR ( $\text{DMSO}-d_6$ )  $\delta$  (ppm): 17.67, 22.12, 26.43, 27.31, 28.98, 49.66, 50.14, 61.94, 67.69, 69.44, 105.75, 110.12, 112.50, 116.00, 116.95, 117.85, 120.49, 122.10, 122.52, 125.63, 125.80, 126.42, 126.77, 126.97, 128.03, 130.91, 134.68, 136.90, 137.36, 137.64, 144.63, 146.78, 147.16, 148.51, 152.00, 154.07, 154.62, 154.86, 155.07, 155.39. UV-vis (DMF, 0.02 mg/mL):  $\lambda_{\text{max}}$  (nm): 484.

**Polymer P5.** Polymer **P1** (89 mg), **5** (47 mg, 0.18 mmol). Deep red powder (112 mg, 87.1%).  $M_w = 10\,100$ ,  $M_w/M_n = 1.28$  (GPC, polystyrene calibration). IR (thin film),  $\nu$  ( $\text{cm}^{-1}$ ): 1716 (C=O), 1517, 1334 ( $-\text{NO}_2$ ).  $^1\text{H}$  NMR ( $\text{DMSO}-d_6$ )  $\delta$  (ppm): 1.6–1.8 ( $-\text{CH}_2-$ ), 1.9–2.2 ( $-\text{CH}_2-$  and  $-\text{CH}_3$ ), 2.7–2.9 ( $-\text{CH}_2-\text{C}-$ ), 3.7–3.9 ( $-\text{N}-\text{CH}_2-$ ), 4.1–4.4 ( $-\text{O}-\text{CH}_2-$  and  $-\text{N}-\text{CH}_2-$ ), 6.8–7.2 (ArH), 7.3–7.4 (ArH), 7.4–7.6 (ArH), 7.6–7.9 (ArH), 7.9–8.1 (ArH), 8.8–9.0 ( $-\text{NH}-$ ), 9.4–9.5 ( $-\text{NH}-$ ).  $^{13}\text{C}$  NMR ( $\text{DMSO}-d_6$ )  $\delta$  (ppm): 8.09, 13.34, 17.70, 22.06, 26.06, 27.96, 28.95, 42.19, 49.44, 50.14, 61.95, 69.26, 109.76, 112.48, 115.97, 116.97, 117.79, 119.33, 120.87, 122.50, 122.68, 126.27, 126.45, 130.93, 136.90, 137.34, 137.65, 140.50, 144.57, 146.68, 147.02, 148.47, 152.00, 154.07, 154.87, 155.09, 155.36. UV-vis (DMF, 0.02 mg/mL):  $\lambda_{\text{max}}$  (nm): 485.

**Polymer P7.** Polymer **P6** (90 mg), **2** (23 mg, 0.18 mmol). Orange red powder (98 mg, 91.6%).  $M_w = 6700$ ,  $M_w/M_n = 1.33$  (GPC,

polystyrene calibration). IR (thin film),  $\nu$  ( $\text{cm}^{-1}$ ): 1719 ( $\text{C}=\text{O}$ ), 1317, 1130 ( $-\text{SO}_2$ ).  $^1\text{H}$  NMR ( $\text{DMSO}-d_6$ )  $\delta$  (ppm): 0.7–0.9 ( $-\text{CH}_3$ ), 1.0–1.4 ( $-\text{CH}_2\text{CH}_2-$ ), 1.6–2.2 ( $-\text{CH}_2-$  and  $-\text{CH}_3$ ), 2.6–2.8 ( $-\text{CH}_2\text{C}-$ ), 3.7–3.9 ( $-\text{N}-\text{CH}_2-$ ), 4.1–4.4 ( $-\text{O}-\text{CH}_2-$  and  $-\text{N}-\text{CH}_2-$ ), 6.9–7.2 (ArH), 7.4–7.6 (ArH), 7.6–8.0 (ArH), 8.8–9.0 ( $-\text{NH}-$ ), 9.4–9.5 ( $-\text{NH}-$ ).  $^{13}\text{C}$  NMR ( $\text{DMSO}-d_6$ )  $\delta$  (ppm): 13.30, 14.40, 17.70, 22.51, 23.18, 24.06, 26.13, 30.21, 31.18, 49.88, 50.16, 55.03, 61.96, 112.51, 116.20, 122.59, 123.06, 126.35, 129.69, 130.93, 136.91, 137.37, 137.64, 139.40, 143.83, 146.03, 152.23, 154.09, 154.87, 155.08, 156.12. UV–vis (DMF, 0.02 mg/mL):  $\lambda_{\text{max}}$  (nm): 445.

**Polymer P8.** Polymer **P6** (90 mg), **3** (24 mg, 0.18 mmol). Orange red powder (92 mg, 83.6%).  $M_w = 6700$ ,  $M_w/M_n = 1.31$  (GPC, polystyrene calibration). IR (thin film),  $\nu$  ( $\text{cm}^{-1}$ ): 1719 ( $\text{C}=\text{O}$ ), 1316, 1129 ( $-\text{SO}_2$ ).  $^1\text{H}$  NMR ( $\text{DMSO}-d_6$ )  $\delta$  (ppm): 1.7–2.2 ( $-\text{CH}_3$  and  $-\text{CH}_2-$ ), 2.6–2.8 ( $-\text{CH}_2\text{C}-$ ), 3.7–3.9 ( $-\text{N}-\text{CH}_2-$ ), 4.2–4.4 ( $-\text{O}-\text{CH}_2-$ ), 5.4–5.6 ( $-\text{CH}_2\text{Ph}$ ), 6.9–7.4 (ArH), 7.5 (ArH), 7.7–8.0 (ArH), 8.8–9.0 ( $-\text{NH}-$ ), 9.4–9.5 ( $-\text{NH}-$ ).  $^{13}\text{C}$  NMR ( $\text{DMSO}-d_6$ )  $\delta$  (ppm): 13.33, 17.75, 23.16, 24.03, 50.16, 53.40, 54.97, 61.96, 112.49, 116.03, 123.10, 125.99, 126.40, 128.47, 128.70, 129.37, 129.73, 130.96, 136.80, 137.36, 137.66, 139.31, 143.76, 146.47, 152.11, 154.10, 154.9, 155.10, 156.07. UV–vis (DMF, 0.02 mg/mL):  $\lambda_{\text{max}}$  (nm): 444.

**Polymer P9.** Polymer **P6** (60 mg), **4** (31 mg, 0.12 mmol). Orange red powder (75 mg, 89.6%).  $M_w = 7200$ ,  $M_w/M_n = 1.40$  (GPC, polystyrene calibration). IR (thin film),  $\nu$  ( $\text{cm}^{-1}$ ): 1723 ( $\text{C}=\text{O}$ ), 1317, 1125 ( $-\text{SO}_2$ ).  $^1\text{H}$  NMR ( $\text{DMSO}-d_6$ )  $\delta$  (ppm): 1.6–2.2 ( $-\text{CH}_2-$  and  $-\text{CH}_3$ ), 3.6–3.9 ( $-\text{N}-\text{CH}_2-$ ), 4.0–4.4 ( $-\text{O}-\text{CH}_2-$  and  $-\text{N}-\text{CH}_2-$ ), 6.7–7.2 (ArH), 7.2–7.6 (ArH), 7.6–8.1 (ArH), 8.8–9.0 ( $-\text{NH}-$ ), 9.4–9.6 ( $-\text{NH}-$ ).  $^{13}\text{C}$  NMR ( $\text{DMSO}-d_6$ )  $\delta$  (ppm): 13.34, 17.73, 23.22, 24.08, 26.44, 27.34, 49.72, 50.17, 54.98, 61.96, 67.71, 105.81, 112.48, 116.10, 120.53, 122.14, 122.73, 123.10, 125.62, 125.91, 126.41, 126.85, 127.05, 128.11, 129.75, 130.99, 134.70, 137.38, 139.32, 143.76, 146.15, 152.21, 154.10, 154.64, 155.10, 156.07. UV–vis (DMF, 0.02 mg/mL):  $\lambda_{\text{max}}$  (nm): 446.

**Polymer P10.** Polymer **P6** (90 mg), **5** (48 mg, 0.18 mmol). Orange red powder (114 mg, 87.8%).  $M_w = 6300$ ,  $M_w/M_n = 1.37$  (GPC, polystyrene calibration). IR (thin film),  $\nu$  ( $\text{cm}^{-1}$ ): 1719 ( $\text{C}=\text{O}$ ), 1317, 1125 ( $-\text{SO}_2$ ).  $^1\text{H}$  NMR ( $\text{DMSO}-d_6$ )  $\delta$  (ppm): 1.6–1.9 ( $-\text{CH}_2-$ ), 1.9–2.2 ( $-\text{CH}_3$  and  $-\text{CH}_2-$ ), 2.6 ( $-\text{CH}_2-$ ), 3.4 ( $-\text{SO}_2\text{CH}_2-$ ), 3.7–3.9 ( $-\text{N}-\text{CH}_2-$ ), 4.2–4.4 ( $-\text{O}-\text{CH}_2-$  and  $-\text{N}-\text{CH}_2-$ ), 6.9–7.2 (ArH), 7.3–7.4 (ArH), 7.4–7.6 (ArH), 7.7–8.0 (ArH), 8.0–8.2 (ArH), 8.8–9.0 ( $-\text{NH}-$ ), 9.4–9.5 ( $-\text{NH}-$ ).  $^{13}\text{C}$  NMR ( $\text{DMSO}-d_6$ )  $\delta$  (ppm): 13.35, 23.16, 24.01, 26.07, 27.94, 42.25, 49.46, 50.19, 54.97, 61.95, 109.82, 112.46, 119.36, 120.89, 122.71, 123.06, 126.32, 129.69, 136.91, 137.35, 139.30, 140.55, 143.76, 146.01, 152.15, 154.20, 154.87, 155.10, 156.06. UV–vis (DMF, 0.02 mg/mL):  $\lambda_{\text{max}}$  (nm): 447.

## 2.5. Preparation of polymer thin films

The polymers were dissolved in THF (concentration  $\sim 3$  wt%) and the solutions were filtered through syringe filters. Polymer films were spin-coated onto indium-tin-oxide (ITO)-coated glass substrates, which were cleaned by DMF, acetone, distilled water and THF sequentially in ultrasonic bath before use. Residual solvent was removed by heating the films in a vacuum oven at 40 °C.

## 2.6. NLO measurement of poled films

The second-order optical nonlinearity of the polymers was determined by in situ second harmonic generation (SHG) experiment using a closed temperature-controlled oven with optical windows and three needle electrodes. The films were kept at 45 °C to the incident beam and poled inside the oven, and the SHG intensity was monitored simultaneously. Poling conditions were as follows: temperature: different for each polymer (Table 1); voltage: 7.5 kV at the needle point; gap distance: 0.8 cm. The SHG measurements were carried out with a Nd:YAG laser operating at a 10 Hz repetition rate and an 8 ns pulse width at 1064 nm. A Y-cut quartz crystal served as the reference.

## 3. Results and discussion

### 3.1. Synthesis

Chromophores **1** and **6** were synthesized through the normal azo coupling reaction with satisfied yields as reported previously [30]. Under the typical polymerization conditions for polyurethanes [36,37], the mother polymers, **P1** and **P6**, were easily obtained, which contained end alkyne groups for the further functionalization. Then, as demonstrated in Schemes 1 and 2, **P2–P5** and **P7–P10** were prepared by the “click” reaction between **P1** or **P6** and the azido-bearing compounds **2–5**, conveniently. In the literatures, generally, polymers bearing azido groups, and functional groups with end alkyne moieties were introduced to the polymer backbone by the copper catalyzed Huisgen cycloaddition. In our case, it was more difficult to prepare the mother polymers with structure similar to **P1** and **P6** but containing azido groups instead of alkyne ones: (1) it was much easier to prepare monomers **1** and **6**, and more difficult to synthesize similar monomers with azido groups; (2) monomers with azido groups might react with other moieties during the polymerization process.

**Table 1**  
Polymerization results and characterization data.

No.	Yield (%)	$M_w^a$	$M_w/M_n^a$	$\lambda_{\text{max}}^b$ (nm)	$T_g^c$ (°C)	$T_d^d$ (°C)	$T^e$ (°C)	$l_s^f$ ( $\mu\text{m}$ )	$d_{33}^g$ (pm/V)	$d_{33(\infty)}^h$ (pm/V)
<b>P1</b>	85.6	15 000	1.49	484	120	272	120	0.34	60.9	8.3
<b>P2</b>	91.6	12 000	1.69	485	93	245	90	0.35	60.3	8.1
<b>P3</b>	87.2	11 200	1.70	485	119	255	129	0.34	64.4	8.6
<b>P4</b>	84.0	12 800	1.40	484	126	252	130	0.30	94.4	13.0
<b>P5</b>	87.1	10 100	1.28	485	127	259	138	0.32	64.0	8.5
<b>P6</b>	88.3	8200	1.60	446	132	284	129	0.26	64.6	15.8
<b>P7</b>	89.7	6700	1.33	445	109	279	109	0.32	73.6	18.2
<b>P8</b>	83.6	6700	1.31	444	128	270	140	0.19	83.8	21.0
<b>P9</b>	89.6	7200	1.40	446	122	279	111	0.46	27.7	6.8
<b>P10</b>	87.8	6300	1.37	447	131	262	140	0.46	11.1	2.7

<sup>a</sup> Determined by GPC in THF on the basis of a polystyrene calibration.

<sup>b</sup> The maximum absorption wavelength of polymer solutions in DMF.

<sup>c</sup> Glass transition temperature ( $T_g$ ) of polymers detected by the DSC analyses under nitrogen at a heating rate of 10 °C/min.

<sup>d</sup> The 5% weight loss temperature of polymers detected by the TGA analyses under nitrogen at a heating rate of 10 °C/min.

<sup>e</sup> The best poling temperature.

<sup>f</sup> Film thickness.

<sup>g</sup> Second harmonic generation (SHG) coefficient.

<sup>h</sup> The nonresonant  $d_{33}$  values calculated by using the approximate two-level model.

However, the usage of mother polymers with end alkyne groups instead of azido groups, caused another problem: how to determine the end point of the reaction between the polymer and the azido compounds, since the absorption peak of end alkyne groups in the FT-IR spectrum is not so strong as that of azido ones. Thus, in the synthetic procedure of polymers **P2–P5** and **P7–P10**, the reaction time was determined to be 3 h according to our previous cases [21,30], in which the reaction progress could be monitored by the FT-IR spectrum. As confirmed by the structure characterization, all the end alkyne groups in polymers **P1** and **P6** underwent the click-chemistry reaction to yield their derivative polymers with the structure shown in Schemes 1 and 2. We would discuss this point in Section 3.2. Actually, we have tried to introduce different isolation groups to the chromophore moieties in polymers through the post-esterification reaction [33], however, the results were not so perfect as the designed reactive groups in the polymer intermediate, hydroxyl ones, could not react with the added small acid molecules completely. This defect led to the comparing of the NLO effects of the resultant polymer not on the same level and some other drawbacks. However, here, thanks to the powerful “click” chemistry, the reaction conducted completely, avoiding the flaw encountered previously. Perhaps, it is the first time that the “click” chemistry reaction is used as the post-functionalization method in the modification of the subtle polymer structure through polymer reactions.

The overall synthetic route was very simple, and different isolation groups could be easily linked to the chromophore moieties in **P1** or **P6** to adjust the subtle structure of the resultant polymers. Thus, in the two series of polymers, **P2–P5** and **P7–P10**, respectively, the main structure was similar and the difference was the different isolation groups introduced. Since there were no conjugated bridges between the isolation spacers and the chromophore moieties, the added isolation groups would not affect the electronic property of the push–pull structure of the chromophore moieties. So, we could ascribe the difference of the tested NLO effects of the resultant polymers to the influence of the bonded different isolation spacers, and explore the suitable isolation group for these two systems.

### 3.2. Structure characterization

The polymers were characterized by spectroscopic methods, and all gave satisfactory data (see Section 2 and Table 1 for detailed data). In all the FT-IR spectra of **P1–P10**, a strong absorption peak at about  $1720\text{ cm}^{-1}$  was attributed to the vibration of the carbonyl groups in the backbone of polyurethane. In the spectra of **P1–P5**, the strong absorption band peaked at about  $1338\text{ cm}^{-1}$  indicated the presence of nitro groups; while the typical signal of sulfonyl moieties was observed at about  $1130\text{ cm}^{-1}$  in those of **P6–P10**. Although, there should be an absorption band derived from the  $\equiv\text{C–H}$  stretching vibrations centred at  $3296\text{ cm}^{-1}$ , the absorption of N–H bonds in the polymer backbone shaded this band. Thus, we could not monitor the progress of the post-click reaction on the change of the absorption peak of the  $\equiv\text{C–H}$  bonds. And from the FT-IR spectra, we could not know if all the  $\equiv\text{C–H}$  groups reacted with azido moieties completely. However, this problem could be solved by analyzing their NMR spectra carefully.

In all the  $^1\text{H}$  NMR spectra of the polymers, the chemical shifts were consistent with the proposed polymer structures demonstrated in Schemes 1 and 2. Fig. 1 showed the  $^1\text{H}$  NMR spectra of **P1** and **P5** for examples. Although, we could not determine if all the end alkyne groups in polymers reacted with the azido moieties completely from their FT-IR spectra, the information obtained in the  $^1\text{H}$  NMR spectra could answer this question. As shown in Fig. 1, the absorption peak of the methylene groups linked to the end alkyne moieties in **P1** was at about 2.36 ppm, however, this peak

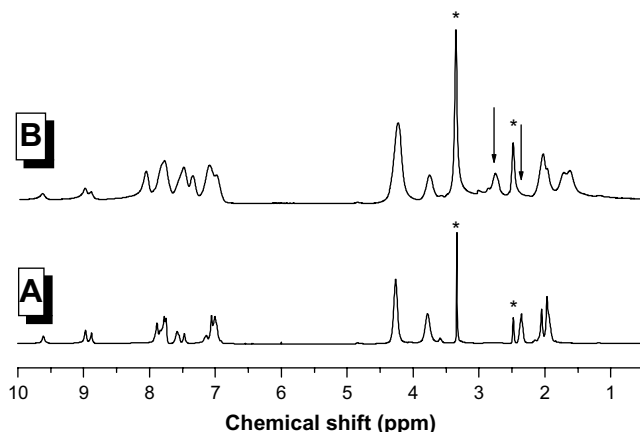


Fig. 1.  $^1\text{H}$  NMR spectra of polymers **P1** (A) and **P5** (B) in  $\text{DMSO-}d_6$ . The solvent peaks were marked with asterisks (\*).

disappeared completely in the  $^1\text{H}$  NMR spectrum of **P5**, but a new peak appeared at about 2.74 ppm, which should be ascribed to the methylene groups bonded to the new formed triazole ring in **P5**. This confirmed that all the alkyne groups have reacted with the added azido moieties, and the structure of **P5** was exactly that demonstrated in Scheme 1. Similar phenomena were also observed in the spectra of other polymers, indicating that their structures were those shown in Schemes 1 and 2. We also conducted the  $^{13}\text{C}$  NMR spectra of all the polymers, and the signal peaks of the alkyne groups at about 72 and 84 ppm in **P1** and **P6**, could not be found in other polymers any longer (**P2–P5** and **P7–P10**), further confirming the completed reaction of the alkyne groups with the added azido moieties.

All the polymers were soluble in common organic solvents, such as THF, DMF and DMSO. Their solutions could be easily spin-coated into thin solid films, therefore, it was convenient to test their NLO properties based on the thin films. The UV–vis absorption spectra were shown in Fig. 2, and the maximum absorption wavelength for the  $\pi\text{--}\pi^*$  transition of the azo moieties in them is listed in Section 2 and Table 1. After the isolation spacers bonded into the polymeric side chain, the maximum absorption wavelength of each kind of polymers with nitro or sulfonyl as acceptors did not change, further confirming that the presence of the different isolation spacers did not influence the electronic properties of the chromophore moieties, which would assure the comparison of their NLO properties on the same level. In comparison with **P1–P5**, **P6–P10** exhibited much blue-shifted maximum absorption wavelength in the same solvent, in accordance with those reported in the literature [38,39]. This point would surely lead to the good transparency of **P6–P10**, and benefit their practical applications by cutting off the optical loss.

The molecular weights of polymers were determined by gel permeation chromatography (GPC), with THF as an eluent and polystyrene standards as calibration standards. All the results are summarized in Table 1. As polymers were derived from **P1** or **P6** by using the post-click-chemistry strategy, most of them possessed similar molecular weights. This would facilitate the comparison of their properties on the same level. The polymers were thermally resistant. Their TGA thermograms are shown in Figs. 3 and 4, and the 5% weight loss temperature of polymers is listed in Table 1. The results showed that all the polymers exhibited good thermal stability up to  $250\text{ }^\circ\text{C}$ . Among them, **P1** and **P6** demonstrated even better thermal stability than their derivatives, respectively. The reason might be that there were end alkyne groups present in **P1** and **P6**, which could undergo thermal crosslinking upon moderate heating [40]. The stability of **P6** was a little higher than that of **P1**, perhaps, indicating that the extent of the thermal reactions



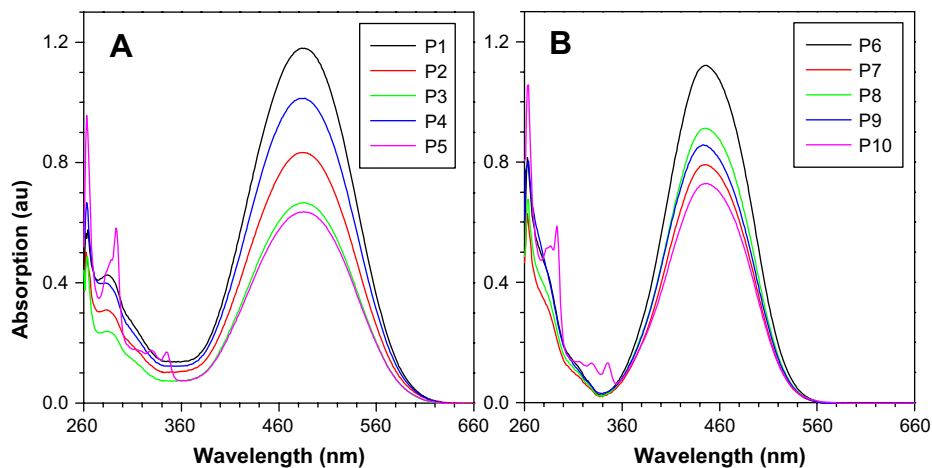


Fig. 2. UV-vis spectra of DMF solutions of polymers (A) **P1–P5**, (B) **P6–P10**. Concentration: 0.02 mg/mL.

between the triple bonds in **P6** was larger than that in **P1**, since the acetylenic groups in **P6** should be more likely exposed outside the polymer chain to react with each other.

The glass transition temperature ( $T_g$ ) of the polymers was investigated using a Setaram differential scanning calorimeter (Table 1). After bonding Hx groups, the  $T_g$  of **P2** and **P7** was lower than that of their mother polymers, **P1** and **P6**, respectively. All the other polymers exhibited similar  $T_g$  as their mother polymer.

### 3.3. NLO properties

To evaluate the NLO activity of the polymers, their poled thin films were prepared. The most convenient technique to study the second-order NLO activity was to investigate the second harmonic generation (SHG) processes characterized by  $d_{33}$ , an SHG coefficient. To check the reproducibility, we repeated the measurements several times for each sample. The method for the calculation of the SHG coefficients ( $d_{33}$ ) for the poled films has been reported in our previous papers [34,35]. From the experimental data, the  $d_{33}$  values of polymers were calculated at 1064 nm fundamental wavelength (Table 1).

Since the two series of polymers, **P1–P5** and **P6–P10**, were derived from the two mother polymers, **P1** and **P6**, respectively, we could analyze their NLO properties nearly on the same level. Also, because the big difference of the polymers in the same series was the different isolation groups, and the presence of the isolation one did not affect the electronic properties of the chromophore moieties in polymers, we could focus our eyes on the effect of the different isolation spacers. As demonstrated by the obtained NLO results, the introduced isolation groups led to the different NLO effects of the resultant polymers.

To study the NLO results visually, we compared the  $d_{33}$  values of the polymers using that of **P1** for **P1–P5** and **P6** for **P6–P10** as reference (the two labeled A curves in Fig. 5). It was seen that the  $d_{33}$  values were not always increasing as the isolation groups enlarged from **P1** (or **P6**) to **P5** (or **P10**). For **P1–P5**, the best isolation spacer was naphthalene group, which made the  $d_{33}$  value of **P4** 1.55 times that of **P1**. Similar phenomena were found in the system of **P6–P10**: the  $d_{33}$  value of **P8** was the highest, in which the isolation spacer was benzyl group. The results were not strange, since the introduced isolation groups mainly caused three impacts:

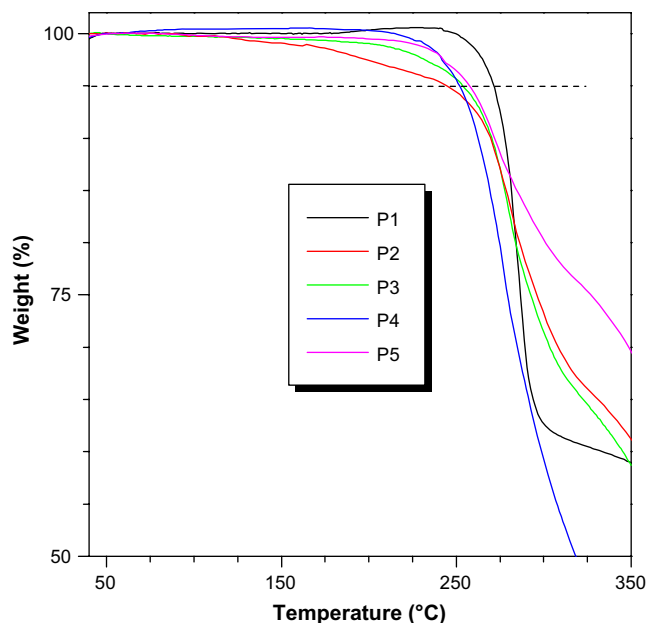


Fig. 3. TGA thermograms of **P1–P5** measured in nitrogen at a heating rate of 10 °C/min.

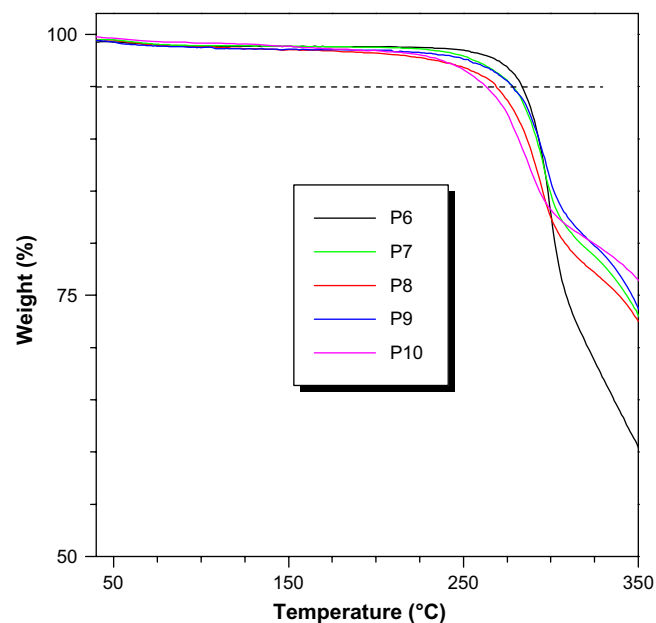
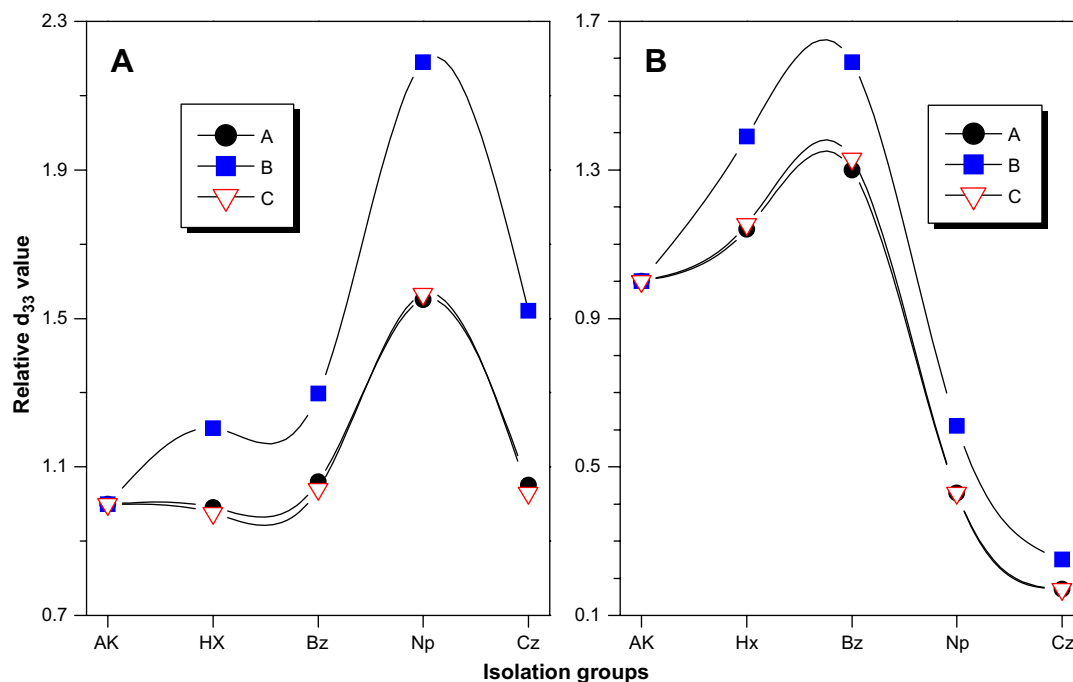


Fig. 4. TGA thermograms of **P6–P10** measured in nitrogen at a heating rate of 10 °C/min.



**Fig. 5.** The analysis of the obtained NLO data of polymers (A) **P1–P5** and (B) **P6–P10**. (A) Comparison of the  $d_{33}$  values of the polymers; (B) comparison of the calculated  $d_{33}$  values, which were obtained by using the tested  $d_{33}$  values dividing the concentration of the active chromophore moieties of the polymers; (C) comparison of the calculated  $d_{33(\infty)}$  values according to the approximate two-level model, using **P1** for **P1–P5**, and **P6** for **P6–P10** as references.

(1) to minimize the strong intermolecular dipole–dipole interactions to some degree, leading to the improvement of the  $d_{33}$  values of the polymers; (2) to dilute the active concentration of the chromophore moieties, generally reducing the  $d_{33}$  values; (3) to increase the bulky of the resultant chromophore moieties, making the noncentrosymmetric alignment of the chromophore upon poling in the electronic field more difficult, which would generate complicated effects on the resultant  $d_{33}$  values (at the beginning, the enlargement of the size would benefit the alignment due to the minimized electrostatic interaction, but would restrain the alignment when the size was too bulky). Thus, the tested NLO results indicated that there was a suitable isolation group for the special chromophore moieties to balance the above-mentioned three effects, with the purpose to boost the fixed microscopic  $\beta$  value of the chromophore moieties to possibly higher macroscopic NLO property in polymers efficiently. As the chromophore moieties and the linkage position in the two series of polymers, **P1–P5** and **P6–P10**, were different, the suitable isolation groups were different for them.

Considering that the introduction of different isolation groups would result in the diluted concentration of the active chromophore moieties in the polymers, we used the tested  $d_{33}$  values dividing the molar concentrations of the active chromophore moieties, then compared the results again with that of **P1** or **P6** as the reference (the two labeled B curves in Fig. 5). It was easily seen that the trend of the two curves (the labeled A and B) was nearly the same, further proving the hypothesis of “the suitable isolation groups”.

Although, as discussed above, the different isolation groups linked to the chromophore moieties would not influence its  $\beta$  value, as confirmed by their nearly the same maximum absorptions observed in the UV–vis spectra, there might be some resonant enhancement due to the absorption of the chromophore moieties at 532 nm. Then, the NLO properties of **P1–P10** should be smaller as shown in Table 1 ( $d_{33(\infty)}$ ), which were calculated by using the approximate two-level model. Also, we drew the curve, still using those of **P1** and **P6** as references (Fig. 5C), and this time, the trend

existing in the  $d_{33(\infty)}$  values was similar as the previous two, nearly overlapping with curve A due to their similar maximum absorptions.

Therefore, by comparing the obtained NLO effects of the polymers from different point of view, we could conclude that really, “the suitable isolation group hypothesis” did work in the reported polymer systems here. Thus, it was reasonable for us to obtain better NLO polymers with even larger macroscopic NLO effects by introducing suitable isolation group to good chromophore moieties reported so far, and further study is still in progress in our lab.

It was very interesting that **P6** exhibited a little higher  $d_{33}$  value than that of **P1**, though the microscopic  $\beta$  value of the sulfonyl-based chromophore moieties in **P6** was smaller than that of the chromophore moieties in **P1** with nitro groups as the acceptor. To analyze their structure in detail, we could find some clues for the possible reasons. Both of these two polymers contained end alkyne groups, which could undergo thermal polymerization upon moderate heating [40]. Just this thermal curing may play an important role in boosting the  $d_{33}$  value of **P6** to a higher point. As we know, in NLO polymers, the noncentrosymmetric alignment of the chromophore upon poling in the electronic field should be achieved, to assure their NLO activity. In the poling process, the thin films of the NLO polymer should be heated to help the noncentrosymmetric alignment of the chromophore moieties, for example, the best poling temperatures of **P1** and **P6** were 120 and 129 °C, respectively. Under these temperatures, the acetylenic triple bonds readily underwent thermal polymerization. Then, in the poling process, the external electronic field would lead to the noncentrosymmetric alignment of the chromophore moieties, meanwhile, the end alkyne groups would react with each other. From the viewpoint of the topological structure of **P1** and **P6**, the thermal reactions between the triple bonds should be easier in **P6** than in **P1**, since the acetylenic groups in **P6** should be more likely exposed outside the polymer chain. As the donor side of the chromophore moieties was inserted into the polymer backbone, the crosslink reaction of the neighbored triple bonds should benefit the noncentrosymmetric alignment of the chromophore

moieties, directly leading to the possibly larger NLO effect. Thus, the relatively higher degree of the crosslink reaction in **P6**, as mentioned above in the discussion part of their thermal stability, should enhance its NLO effects in a larger degree, even higher than that of **P1**. Also, the relatively higher degree of the crosslink reaction in **P6** rather than in **P1** could be further partially confirmed by their dynamic thermal stabilities of the NLO activities, and we would discuss this point in the following part.

In 2006, we prepared polymers with the same structure as **P2–P5**, from the direct copolymerization of their corresponding monomers [22]. The obtained results demonstrated that the best isolation spacer in this polymer system was benzyl group, different from the naphthalene group reported here. This was very strange at the first glance, however, might indicate that the poling efficiencies and the macroscale NLO properties of polymers containing dendronized chromophore as side groups were heavily related to the subtle difference in architectural design, as reported in the literature [23,41,42], since the subtle structure of the polymers from the copolymerization process should be different from that obtained through polymer reactions. Thus, this phenomenon might prove that we could adjust the subtle structure of polymers through post-functionalization strategy, possibly another advantage of post-functional route. If so, there should be another way for the scientists to control the property of their synthesized polymeric materials. Further work should be done to confirm this standpoint.

The dynamic thermal stabilities of the NLO activities of the polymers were investigated by the depoling experiments, in which the real time decays of their SHG signals were monitored as the poled films were heated from 40 to 160 °C in air at a rate of 4 °C/min. As shown in Fig. 6, the polymers with nitro as acceptors possess relatively good long-term temporal stability with the onset temperatures for decays in the  $d_{33}$  values around 120 °C, in accordance with those observed previously. However, the stability of **P1** and **P6** was similar to or better than their derivative polymers. The main reason should be the presence of alkyne groups, which might undergo thermal crosslinking process as discussed above. The onset temperature for the decay of the  $d_{33}$  value of **P6** was about 126 °C, higher than that of **P1** (120 °C), indicating the higher degree of the crosslink reaction in **P6** rather than in **P1**. Thus, the end alkyne

groups in polymers could offer the opportunity for the post-processing of the polymers to improve their stability.

#### 4. Conclusion

By using “click” chemistry, different isolation groups were conveniently introduced into the chromophores of polymers to yield two series of NLO polyurethanes with adjustable subtle structure. The synthesized polymers were well characterized, and easily soluble in common organic solvents. Our preliminary study demonstrated that the NLO results further confirmed that there was “a suitable isolation group” present for a chromophore to boost its microscopic  $\beta$  value to possibly higher macroscopic NLO property in polymers efficiently. The successful example for the preparation of functional polymers reported here demonstrated the power of “Click Chemistry”, and it is believed that the subtle structure of other functional polymers could be modified by using this strategy through polymer reactions conveniently. The good NLO properties of **P1–P10**, coupled with their good thermal stability, offered them good candidates for the practical photonic applications. And the presence of the crosslinkable alkyne groups provided the additional enhanced thermal stability of **P1** and **P6**, based on this point, we could design some other NLO polymers with even better stability.

#### Acknowledgements

We are grateful to the National Science Foundation of China (no. 20674059), the National Fundamental Key Research Program and Hubei Province for financial support.

#### References

- [1] Rostovtsev VV, Green LG, Fokin VV, Sharpless KB. A stepwise Huisgen cycloaddition process: copper(I)-catalyzed regioselective “ligation” of azides and terminal alkynes. *Angewandte Chemie International Edition* 2002;41:2596–9.
- [2] Helms B, Mynar JL, Hawker CJ, Fréchet JM. Dendronized linear polymers via “Click Chemistry”. *Journal of American Chemical Society* 2004;126:15020–1.
- [3] Binder WH, Sachsenhofer R. Review ‘Click’ chemistry in polymer and materials science. *Macromolecular Rapid Communications* 2007;28:15–54.
- [4] Lutz JF. 1,3-Dipolar cycloadditions of azides and alkynes: a universal ligation tool in polymer and materials science. *Angewandte Chemie International Edition* 2007;46:1018–25.
- [5] Ornelas C, Aranzas JR, Cloutet E, Alves S, Astruc D. Click assembly of 1,2,3-triazole-linked dendrimers, including ferrocenyl dendrimers, which sense both oxo anions and metal cations. *Angewandte Chemie International Edition* 2007;46:872–7.
- [6] Qin A, Jim CKW, Lu W, Lam JWY, Häussler M, Dong Y, et al. Click polymerization: facile synthesis of functional poly(aryltriazole)s by metal-free, regioselective 1,3-dipolar polycycloaddition. *Macromolecules* 2007;40:2308–17.
- [7] Gao H, Louche G, Sumerlin BS, Jahed N, Golas P, Matyjaszewski K. Gradient polymer elution chromatographic analysis of  $\alpha,\omega$ -dihydroxypolystyrene synthesized via ATRP and click chemistry. *Macromolecules* 2005;38:8979–82.
- [8] Sumerlin BS, Tsarevsky NV, Louche G, Lee RY, Matyjaszewski K. Highly efficient “Click” functionalization of poly(3-azidopropyl methacrylate) prepared by ATRP. *Macromolecules* 2005;38:7540–5.
- [9] Lutz JF, Börner HG, Weichenhan K. Combining atom transfer radical polymerization and click chemistry: a versatile method for the preparation of end-functional polymers. *Macromolecular Rapid Communications* 2005;26:514–8.
- [10] Wu P, Feldman AK, Nugent AK, Hawker CJ, Scheel A, Voit B, et al. Efficiency and fidelity in a click-chemistry route to triazole dendrimers by the copper(I)-catalyzed ligation of azides and alkynes. *Angewandte Chemie International Edition* 2004;43:3928–32.
- [11] Li C, Finn MG. Click chemistry in materials synthesis. II. Acid-swellable crosslinked polymers made by copper-catalyzed azide–alkyne cycloaddition. *Journal of Polymer Science, Part A: Polymer Chemistry* 2006;44:5513–8.
- [12] Diaz DD, Punna S, Holzer P, McPherson AK, Sharpless KB, Fokin VV, et al. Click chemistry in materials synthesis. 1. Adhesive polymers from copper-catalyzed azide–alkyne cycloaddition. *Journal of Polymer Science, Part A: Polymer Chemistry* 2004;42:4392–403.
- [13] Binder WH, Kluger C. Combining ring-opening metathesis polymerization (ROMP) with Sharpless-type “Click” reactions: an easy method for the preparation of side chain functionalized poly(oxynorbornenes). *Macromolecules* 2004;37:9321–30.
- [14] Sawa M, Hsu TL, Itoh T, Sugiyama M, Hanson SR, Vogt PK, et al. Glycoproteomic probes for fluorescent imaging of fucosylated glycans in vivo. *Proceedings of*

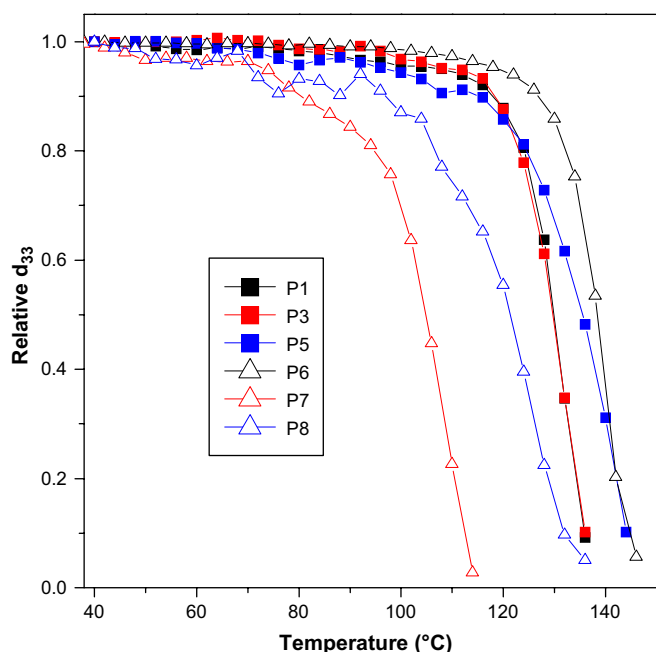


Fig. 6. Decay of SHG coefficient of polymers as a function of temperature.



- the National Academy of Science of the United States of the America 2006;103:12371–6.
- [15] Altintas O, Hizal G, Tunca U. ABC-type hetero-arm star terpolymers through “Click” chemistry. *Journal of Polymer Science, Part A: Polymer Chemistry* 2006;44:5699–707.
  - [16] Li H, Cheng F, Duft AM, Adronov A. Functionalization of single-walled carbon nanotubes with well-defined polystyrene by “Click” coupling. *Journal of American Chemical Society* 2005;127:14518–24.
  - [17] Itsuno S. Chiral polymer synthesis by means of repeated asymmetric reaction. *Progress in Polymer Science* 2005;540–58.
  - [18] O'Reilly RK, Joralemon MJ, Hawker CJ, Wooley KL. Preparation of orthogonally-functionalized core Click cross-linked nanoparticles. *New Journal of Chemistry* 2007;31:718–24.
  - [19] Malkoch M, Schleicher K, Drockenmuller E, Hawker CJ, Russell TP, Wu P, et al. Structurally diverse dendritic libraries: a highly efficient functionalization approach using click chemistry. *Macromolecules* 2005;38:3663–78.
  - [20] O'Reilly RK, Joralemon MJ, Wooley KL, Hawker CJ. Functionalization of micelles and shell cross-linked nanoparticles using click chemistry. *Chemistry of Materials* 2005;17:5976–88.
  - [21] Zeng Q, Li Z, Li Z, Ye C, Qin J, Tang BZ. Convenient attachment of highly polar azo chromophore moieties to disubstituted polyacetylene through polymer reactions by using “click” chemistry. *Macromolecules* 2007;40:5634–7.
  - [22] Li Z, Zeng Q, Li Z, Dong S, Zhu Z, Li Q, et al. An attempt to modify nonlinear optical effects of polyurethanes by adjusting the structure of the chromophore moieties at molecular level using “click” chemistry. *Macromolecules* 2006;39:8544–6.
  - [23] Sullivan PA, Akelaitis AJP, Lee SK, McGrew G, Lee SK, Choi DH, et al. Novel dendritic chromophores for electro-optics: influence of binding mode and attachment flexibility on electro-optic behavior. *Chemistry of Materials* 2006;18:344–51.
  - [24] Ma H, Liu S, Luo J, Suresh S, Liu L, Kang SH, et al. Highly efficient and thermally stable electro-optical dendrimers for photonics. *Advanced Functional Materials* 2002;12:565–74.
  - [25] Kim TD, Luo J, Tian Y, Ka JW, Tucker NM, Haller M, et al. Diels–Alder “click chemistry” for highly efficient electrooptic polymers. *Macromolecules* 2006;39:1676–80.
  - [26] Fréchet JMJ, Hawker CJ, Gitsov I, Leon JW. Dendrimers and hyperbranched polymers: two families of three-dimensional macromolecules with similar but clearly distinct properties. *Journal of Macromolecular Science Part A: Pure and Applied Chemistry* 1996;A33:1399–425.
  - [27] Li Z, Li Z, Di C, Zhu Z, Li Q, Zeng Q, et al. Structural control of the side-chain chromophores to achieve highly efficient nonlinear optical polyurethanes. *Macromolecules* 2006;39:6951–61.
  - [28] Li Q, Li Z, Zeng F, Gong W, Li Z, Zhu Z, et al. From controllable attached isolation moieties to possibly highly efficient nonlinear optical main-chain polyurethanes containing indole-based chromophores. *Journal of Physical Chemistry B* 2007;111:508–14.
  - [29] Li Z, Dong S, Li P, Li Z, Ye C, Qin J. New PVK-based nonlinear optical polymers: enhanced nonlinearity and improved transparency. *Journal of Polymer Science, Part A: Polymer Chemistry* 2008;46:2983–93.
  - [30] Li Z, Zeng Q, Yu G, Li Z, Ye C, Liu Y, et al. New azo chromophore-containing conjugated polymers: facile synthesis by using “click” chemistry and enhanced nonlinear optical properties through the introduction of suitable isolation groups. *Macromolecular Rapid Communications* 2008;29:136–41.
  - [31] Li Z, Yu G, Li Z, Liu Y, Ye C, Qin J. New second-order nonlinear optical polymers containing the same isolation groups: optimized syntheses and nonlinear optical properties. *Polymer* 2008;49:901–13.
  - [32] Li Z, Dong S, Yu G, Li Z, Liu Y, Ye C, et al. Novel second-order nonlinear optical main-chain polyurethanes: adjustable subtle structure, improved thermal stability and enhanced nonlinear optical property. *Polymer* 2007;48:5520–9.
  - [33] Li Z, Li P, Dong S, Zhu Z, Li Q, Zeng Q, et al. Controlling nonlinear optical effects of polyurethanes by adjusting isolation spacers through facile postfunctional polymer reactions. *Polymer* 2007;47:3650–7.
  - [34] Li Z, Huang C, Hua J, Qin J, Yang Z, Ye C. A new postfunctional approach to prepare second-order nonlinear optical polyphosphazenes containing sulfonyl-based chromophore. *Macromolecules* 2004;37:371–6.
  - [35] Li Z, Qin J, Li S, Ye C, Luo J, Cao Y. Polyphosphazene containing indole based dual chromophores: synthesis and nonlinear optical characterization. *Macromolecules* 2002;35:9232–5.
  - [36] Tsutsumi N, Matsumoto O, Sakai W. Orientational relaxation of transversely aligned nonlinear optical dipole moments to the main backbone in the linear polyurethane. *Macromolecules* 1997;30:4584–9.
  - [37] Moon KJ, Shim HK, Lee KS, Zieba J, Parasad PN. Synthesis, characterization, and second-order optical nonlinearity of a polyurethane structure functionalized with a hemicyanine dye. *Macromolecules* 1996;29:861–7.
  - [38] Xu C, Wu B, Dalton LR, Shi Y, Ranan PM, Steier WH. Novel double-end crosslinkable chromophores for second-order nonlinear optical materials. *Macromolecules* 1992;25:6714–5.
  - [39] Ulman A, Willand CS, Kohler W, Robello DR, Williams DJ, Handley L. New sulfonyl-containing materials for nonlinear optics: semiempirical calculations, synthesis, and properties. *Journal of American Chemical Society* 1990;112:7083–90.
  - [40] Yu LP, Chan WK, Bao ZN. Synthesis and characterization of a thermally curable second-order nonlinear optical polymer. *Macromolecules* 1992;25:5609–12.
  - [41] Dalton LR. Organic electro-optic materials. *Pure and Applied Chemistry* 2004;76:1421–33.
  - [42] Luo J, Haller M, Ma H, Liu S, Kim TD, Tian Y, et al. Nanoscale architectural control and macromolecular engineering of nonlinear optical dendrimers and polymers for electro-optics. *Journal of Physical Chemistry B* 2004;108:8523–30.